NATIONAL AERONAUTICS AND SPACE ADMINISTRATION

Technical Report 32-1551

Experimental Evaluation of High-Thrust, Throttleable, Monopropellant Hydrazine Reactors

Robert W. Riebling
Gerhard W. Kruger

JET PROPULSION LABORATORY
CALIFORNIA INSTITUTE OF TECHNOLOGY
PASADENA, CALIFORNIA

March 1, 1972

Prepared Under Contract No. NAS 7-100
National Aeronautics and Space Administration

Preface

The work described in this report was performed by the Propulsion Division of the Jet Propulsion Laboratory.

Acknowledgement

The authors wish to acknowledge the contributions of Theodore W. Price and Robert L. Condon of the Liquid Propulsion Section at JPL and of Allen D. Harper, Richard J. Kenny, and Donald F. Reeves of TRW Systems Group.

Contents

Contents (contd)

Tables

Figures

Contents (contd)

Figures (contd)

Abstract

Throttleable monopropellant hydrazine catalytic reactors of a size applicable to a planetary landing vehicle have been designed, fabricated, and tested. An experimental evaluation of two 2670-N (600-lb_f) reactor designs has been conducted. The steady-state and dynamic characteristics of the thruster/valve combinations have been determined. The results of the testing, including the engine characteristic velocity, smoothness of combustion, insensitivity to heat sterilization, and response during various simulated duty cycles are presented and discussed. No problems of a fundamental nature were encountered as a result of rapid dynamic throttling of these large hydrazine reactors.

Experimental Evaluation of High-Thrust, Throttleable, Monopropellant Hydrazine Reactors

I. Introduction

Several published studies of planetary lander missions (Refs. 1 and 2) as well as numerous unpublished ones have shown significant advantages for throttleable monopropellant hydrazine rocket engines as the devices to provide the terminal velocity correction. Depending on the assumptions, these studies result in the selection of a three- or four-engine configuration, with each engine producing a thrust in the range of 1300 to 4500 N (roughly 300 to 1000 lb_f). For the *Viking* Mars lander, three engines, each capable of 2670-N (600-lb_f) thrust, will be used.

In addition to the inherent superior reliability of monopropellant systems as compared to bipropellants, there were three decisive factors which led to the choice of monopropellant hydrazine for planetary lander missions. These factors, all related to the extraterrestrial life experiments typically planned for such missions, are: (1) an exhaust gas temperature significantly lower than that produced by a bipropellant engine – 1350 K (2000°F) compared to 3000 K (5000°F) – which reduces the likelihood of destroying soil organisms in the vicinity of the landing site; (2) the feasibility of heat sterilization of the entire propulsion system, including the fuel, before launch (Ref. 3); and (3) the presence in the exhaust gases of only small amounts of carbon and water,[1] which are commonly found in the exhaust of bipropellant rocket engines and could easily invalidate or confuse the life experiments planned.

At the time of the inception of the work to be discussed (early 1969), there had been only a limited amount of experience with either high-thrust catalytic hydrazine reactors (arbitrarily defined here as in excess of 900 N (200 lb_f) or throttled catalytic hydrazine reactors of any size. The potential problem areas anticipated at the start of the program fell into two broad categories: those common to all catalytic reactors, and those unique to reactors for lander-type missions. Among problems in the first category were retention of the catalyst, structural support of the catalyst, and adequate distribution of the fuel over the catalyst bed. Included among those in the second category were sterilization and rapid dynamic throttling.

[1]Both are present as impurities in military grade hydrazine (the carbon in the form of aniline) but could be nearly eliminated through further refinement of the hydrazine during processing.

Although none of the potential problem areas appeared likely to require major technology advances, further investigation was deemed advisable in light of the then general industry-wide lack of experience. Therefore, an advanced development program was undertaken at the Jet Propulsion Laboratory (JPL) to investigate the broad technology area of high-thrust, throttleable monopropellant hydrazine reactors. This program consisted of two parts, both under JPL technical direction: an in-house effort and a contracted effort with TRW Systems Group. The in-house program emphasized heavyweight, bolt-up research hardware, while the TRW portion of the work stressed a lightweight flight-type design. The thrusters from both efforts were compatible with flight-weight throttle valves. The TRW portion of the program, hereinafter to be referred to as the "lightweight engine," was completed earlier and the results were reported in Refs. 4 and 5. Those results will be recapitulated here. The lightweight engine was then subjected to additional testing at JPL, and those further results will be presented and discussed here.

Earlier portions of the in-house program have also been reported previously. References 6 and 7 describe several series of tests conducted with subscale, 222-N (50-lb_f) thrust hardware. These tests demonstrated that heat sterilization of a catalytic reactor has no major deleterious effect on subsequent operation, that rapid dynamic throttling of a catalytic reactor is completely feasible, and that extended operating times, even with "cold" 278 K (40°F) propellant, are easily possible for certain catalytic reactors.

This report presents and discusses the results obtained in the entire throttleable hydrazine thruster development program. Primary emphasis, however, will be placed on the presentation of the results of the experimental evaluation of the two high-thrust throttleable thruster designs. Portions of this report were presented earlier as Ref. 8.

II. Approach

This program was divided into subscale and full-scale reactor evaluations. The subscale testing made use of existing 222-N (50-lb_f) thrust *Mariner* 1969 reactors for the heat sterilization experiments, the results of which were expected to be virtually independent of reactor size, and for preliminary throttling evaluations. In this way, much information directly applicable to the design and operation of the larger reactors was obtained at relatively low cost. The full-scale program provided proof-of-principle demonstration and permitted performance evaluation with engine hardware in a size range directly applicable to planetary landers. In addition, it provided a framework within which the design and fabrication of flightweight prototype throttleable hydrazine thrusters could be carried out.

A. Subscale Program

Three 222-N (50-lb_f) thrust *Mariner* Mars 1969 monopropellant hydrazine reactors were used in the subscale tests to determine the effects of heat sterilization, long-duration firings, and dynamic throttling on reactor performance. *Mariner* reactors were chosen for these initial evaluations because they had been thoroughly characterized during flight qualification tests. Since the baseline *Mariner* engine characteristic velocity, pressure drop, operating temperature, and other parameters were well defined, it was felt that the effects of heat sterilization, throttling, and long-duration firings with chilled propellant could be easily detected through departures of the operating parameters from their usual values. It was felt that the results would be applicable to reactors of any size.

Two of the three surplus *Mariner* reactors were used for the sterilization tests. Holding one engine as a control, the other was subjected to a cycle of six, 64-h thermal soaks at 408 K (276°F) in a nitrogen atmosphere. Then both engines were fired to determine the effect of sterilization.

The third *Mariner* engine was modified to incorporate additional instrumentation and catalyst support. Using previously fired catalyst, the engine was then fired with chilled propellants for long periods in a steady-state mode.

Two of the engines were used to investigate dynamic throttling, steady-state performance, dynamic stability, and response characteristics. The reactors were operated from prerecorded tape signals in a step and sinusoidal mode.

B. Full-Scale Program

The full-scale test program was further divided into two parts under JPL technical direction. A heavyweight engine, using design concepts previously proven at a smaller scale, was designed, fabricated and tested in-house. No effort was made to minimize its weight or volume. In the design of this reactor, however, special attention was given to catalyst retention, because previous experience with *Mariner* 1969 engines had indicated that rigid support was necessary to minimize relative motion

of the particles. This grinding action has been known to generate small granules (fines) that can be lost through the retaining screens, thereby degrading engine performance. The heavyweight engine used a stainless steel structure with a showerhead injector and a cylindrical catalyst bed. Again drawing on the *Mariner* experience, the showerhead injector was chosen to promote a uniform fuel distribution. The latter was expected to reduce combustion roughness (average variation in chamber pressure divided by mean chamber pressure), which in turn was expected to maintain a well-packed catalyst bed and reduce catalyst lost as fines. A layered catalyst bed was used. The upstream layer consisted of small particles of the spontaneous Shell 405 catalyst to assure smooth, rapid ignition, while the downstream layer comprised larger pellets of the nonspontaneous HA3 catalyst to sustain the decomposition reaction.

Design, fabrication, and preliminary testing of a lightweight, flight-prototype engine was contracted to TRW Systems Group. This three-phase contract used the then-existing *Viking* lander engine requirements as design goals. The engine was weight-optimized by using an elliptical chamber made of high-strength L605 alloy. The final design incorporated a layered catalyst bed using two discrete sizes of Shell 405 catalyst, with a modified showerhead injector. Fabrication and limited testing of this engine were performed by the contractor. As part of the contracted effort, TRW Systems Group also procured two candidate flight-type throttle valves, characterized one, and delivered both to JPL for further evaluation in conjunction with both full-scale thrusters. Additional testing to determine throttled performance and dynamic response characteristics was then performed at JPL.

III. Apparatus and Procedures

A. Subscale Test Hardware

The *Mariner* 1969 reactors used in the subscale tests incorporated a showerhead injector and a layered catalyst bed. The upper bed contained two layers of 20-30 mesh Shell 405 catalyst, while the lower bed had a mixture of 3.2-mm (1/8-in.) Shell 405 and HA3 pellets. At its rated thrust of 222.4 N (50 lb_f), this cylindrically shaped engine had a bed loading of 33.1 kg/m^2 s (0.047 $lb_m/in.^2$-s). The *Mariner* reactor is diagrammed in Fig. 1 and described at length in Ref. 9. Additional details concerning test setup and hardware may be found in Refs. 6 and 7.

During subscale throttling tests, the engine was operated with a surplus *Surveyor* throttle valve (Ref. 10).

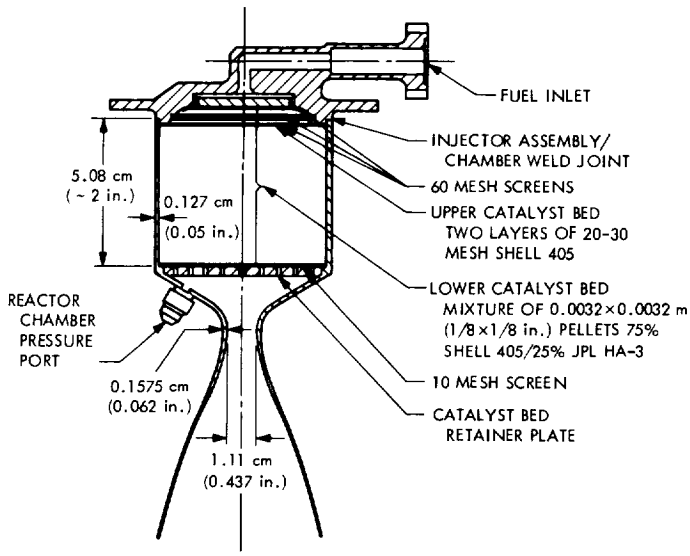

Fig. 1. *Mariner* Mars 1969 engine, internal configuration

Since this was a bipropellant valve of low flow capacity, both sides were flowed in parallel to accommodate the *Mariner* engine flow rate of 0.1 kg/s (0.22 lb_m/s). This reactor/valve system was not intended to represent an optimum performance combination and was used chiefly because of hardware availability.

B. Heavyweight Engine

The heavyweight engine design was based on previous successful monopropellant thruster experience at JPL. As shown in Figs. 2 and 3, it utilized a showerhead injector with two layered catalyst beds: 14-18 mesh Shell 405 in the upper bed and 3.2-mm (1/8-in.) HA3 pellets in the lower bed. Throttling of this engine was accomplished with a variable-area, motor-driven valve to be described subsequently. This engine was a bolt-up, stainless steel design and was fabricated at JPL. The original design parameters are given in Table 1.

This engine design was modified twice during the course of the test program. The first modification increased the depth of the upper catalyst bed from 5.08-mm (0.2 in.) to 7.61-mm (0.3 in.) to improve the start transient behavior.

The second modification involved replacing some of the original bolted joints with brazes and weldments and replacing the upper Marmon clamp with a bolt-up flange to eliminate minor leaks in the chamber. Figure 2 depicts the engine design after the first modification. As shown, the engine was held together with Marmon clamps and had three metal O ring seals. The orifice plate seal

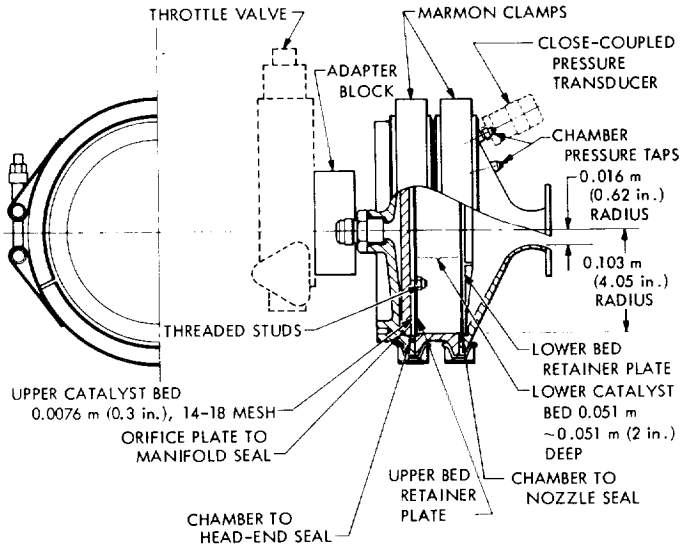

Fig. 2. Original heavyweight engine configuration

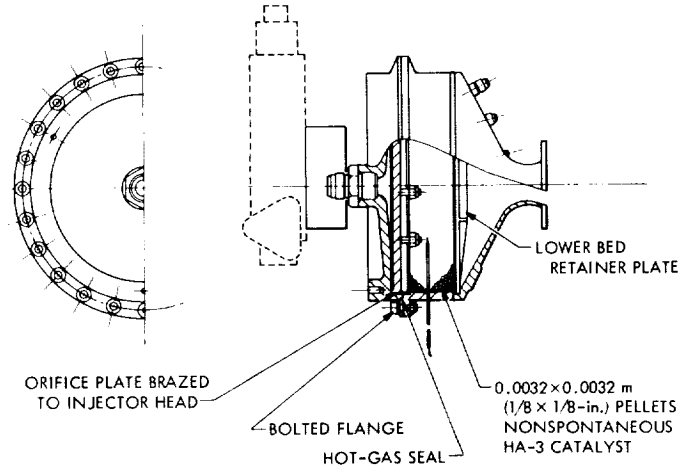

Fig. 3. Modified heavyweight engine configuration

and lower plate retainer seal were eliminated in the second modification. A maximum chamber pressure of 2.07 MN/m² (300 psia) was chosen to assure sonic flow through the nozzle under deep-throttled conditions in sea-level testing. Sixty- and 10-mesh Haynes alloy screens were used to retain the catalyst particles in the upper and lower beds, respectively. Using a showerhead injector with 132 orifices, an injection velocity of 15.23 m/s (50 ft/s) was obtained at full thrust. In its final configuration, this engine required 592 g (1.31 lb_m) of 14-18 mesh Shell 405 catalyst in the upper bed and 1.77 kg (3.9 lb_m) of HA3 below. The final engine configuration is shown in Fig. 3.

Table 1. Heavyweight engine design parameters

Parameter	Value
Full thrust, $\epsilon = 1.5$	2670 N (600 lb_f)
Chamber pressure	2.07 MN/m² (300 psia)
Bed loading	31.6 kg/m² s (0.045 lb_m/in.² s)
Injection velocity	15.23 m/s (50 ft/s)
Throat diameter	31.5 mm (1.24 in.)
Chamber diameter	20.6 cm (8.1 in.)
Upper catalyst bed depth	5.08 mm (0.2 in.) originally; changed to 7.62 mm (0.3 in.)
Lower catalyst bed depth	45.7 mm (1.8 in.)
Upper catalyst screen	60 mesh Haynes 25 (L-605 alloy)
Lower catalyst screen	10 mesh Haynes 25 (L-605 alloy)
Chamber wall thickness	6.67 mm (0.260 in.)
Chamber material	304 stainless steel
Seals	3 metal O rings
Fasteners	3 clamps
Injector	Showerhead 132 orifices 0.787-mm (0.031-in.) diam
Upper catalyst mass	395 g (0.871 lb_m) Shell 405 originally; changed to 592 g (1.31 lb_m)
Lower catalyst mass	1.77 kg (3.9 lb_m) HA3
Upper catalyst size	14-18 mesh
Lower catalyst size	3.2-mm (1/8-in.) pellets
Throttle range	10/1

C. Lightweight Engine

In the lightweight engine design (Ref. 4) care was exercised to reduce both weight and volume. Table 2 summarizes the final design parameters. This engine was also sized for 2670-N (600-lb_f) thrust; however, to minimize thrust chamber weight, a chamber pressure of 1.38 MN/m² (200 psia) was chosen. This was compatible with sonic nozzle flow because it was planned to fire the engine under vacuum conditions. Utilizing an ellipsoidal chamber of L605 material, the loaded thruster weight (less valve) was 5.67 kg (12.5 lb_m). This engine used two layered catalyst beds of Shell 405 catalyst: 14-18 mesh in the upper bed, and 3.2-mm (1/8-in.) pellets in the lower bed. The engine design is depicted in Fig. 4. This engine had two unique features: a hemispherical injector face and a void volume between the injector and the upper bed. This injector configuration was believed by the contractor to improve liquid penetration of the upper bed by the hydrazine jets.

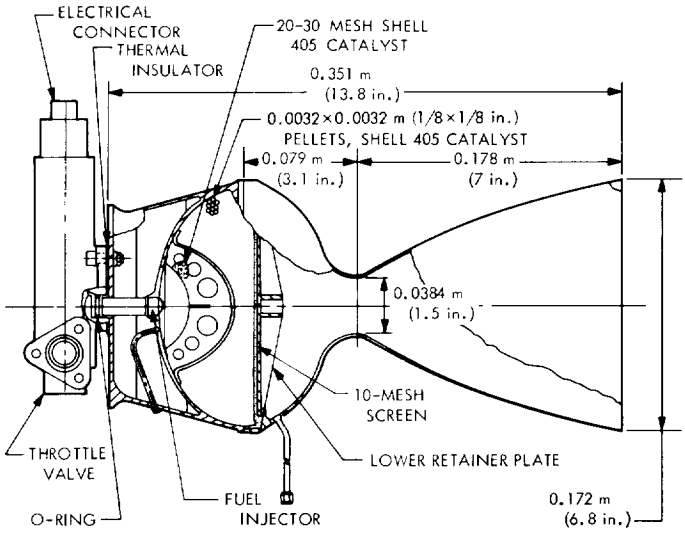

Fig. 4. Lightweight throttleable thruster configuration

In the evolutionary development of this engine, two design modifications were made. First, the catalyst bed geometry was changed from its original configuration of two cylinders concentric with the engine axis to the two concentric spheres centered on the injector face shown in Fig. 4. This change was made to reduce originally encountered engine roughness. The second change replaced the lower catalyst retainer plate design and material. The initial TZM material was replaced by L605 alloy after a brittle failure occurred to the former (Ref. 11). It is believed that the TZM failure resulted from improper processing and was not a consequence of inherent material properties.

Both heavyweight and lightweight thrusters had similar propellant inlet designs, so that both chambers would mate with either of the two throttle valves described below.

D. Throttle Valves

Two candidate throttle valves were evaluated. These valves, hereinafter designated as No. 1 and No. 2, were designed and fabricated by LTV[2] and Moog[3] respectively. The valves are shown schematically in Figs. 5 and 6.

In valve 1, fuel enters the inlet port (upper left), flows through the annular passage between the metering orifice and the pintle, and thence out the outlet port. By linear motion of the tapered pintle, the annular flow passage through the metering orifice can be changed. Pintle motion is effected by an electric-motor-driven ball screw assembly. Pintle position is determined by the linear voltage differential transducer (LVDT) located to the right of the electric motor. Using a feedback loop through the valve driver circuitry (not shown), the pintle position is established by comparison of the sensed position signal and some predetermined set point. The fuel cavity within the valve is sealed with two ethylene-propylene rubber (EPR) dynamic seals and an external static seal. For additional protection, the ball screw/motor assembly and LVDT are isolated from the remainder of the valve by a low-pressure bellows.

The flow path in valve 2 (Fig. 6), is from the inlet port (located on the bottom) into the vane cavity, then between the vane and metering sleeve into the annular cavity, and thence out through the outlet port (right side). Throttling is accomplished by varying the flow passage area between the vane and sleeve. Rotation of the vane uncovers a progressively larger fraction of the metering sleeve slot area, thereby controlling the amount of fuel entering the annulus, and thus leaving the valve. Rotation of the vane is effected via the attached electric motor. The vane position is sensed by a band (not shown on the diagram) wrapped around the vane shaft

Table 2. Lightweight engine design parameters

Parameter	Value
Thrust, $\epsilon = 20$	2670 N (600 lb_f)
Chamber pressure	1.38 MN/m^2 (200 psia)
Nozzle expansion area ratio	20
Throat diameter	38.4 mm (1.513 in.)
Chamber geometry	Ellipsoidal
Characteristic length	1.09 m (43 in.)
Maximum chamber diameter	165 mm (6.5 in.)
Catalyst weight	1.35 kg (2.97 lb_m)
Chamber weight	4.32 kg (9.53 lb_m)
Catalyst type	Upper bed: 14-18 mesh Shell 405 Lower bed: 3.2-mm (1/8-in.) pellets Shell 405
Structural material	L605
Engine design life	500 s
Design throttle range	10/1
Bed loading at maximum chamber diameter, full thrust	63.3 kg/m^2 s (0.09 $lb_m/in.^2$-s)

[2]LTV Electrosystems, Arlington, Texas; P/N 40164400, SN 001.

[3]Moog, Inc., Western Development Center, Monterey Pass, California; P/N 010-32821-2, SN 001.

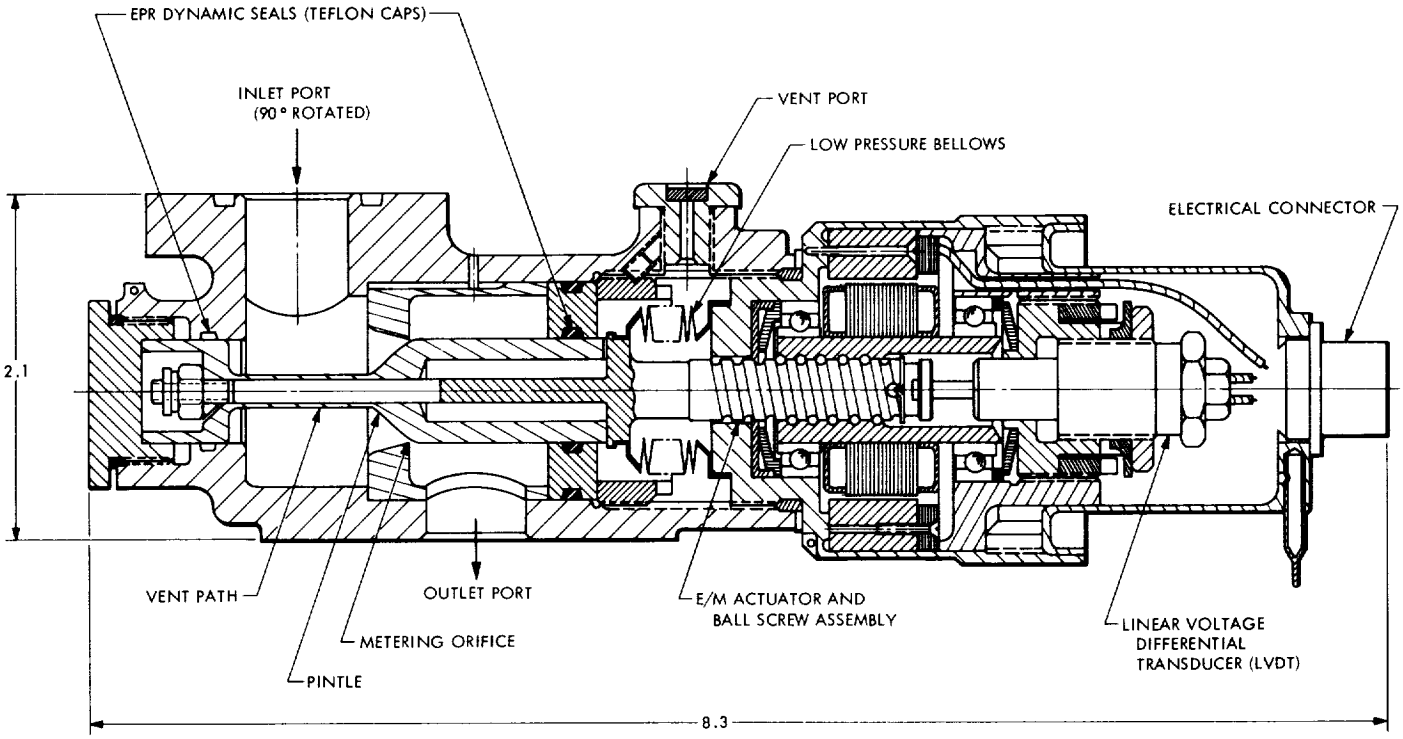

Fig. 5. Throttle valve 1

and attached to an LVDT. As with valve 1, a feedback loop to the valve driver provides ultimate control of flow through the valve. The valve has a completely welded structure with no mechanically sealed joints (the motor armature is exposed to the fuel). This valve features rotary motion of the vane and complete hermetic sealing.

The characteristics of both valves are compared in Table 3, and more detailed descriptions may be found in Refs. 4 and 11.

E. Test Facilities and Instrumentation

All engine testing at JPL was done at sea level. A schematic of the test facility is shown in Fig. 7. The nitrogen-pressurized feed system employed a stainless-steel fuel tank and feed lines. Pressure and temperature measurements were made with standard strain-gauge transducers and chromel–alumel thermocouples respectively. Flow measurements were made with two turbine flow meters in tandem. Instrument calibrations including coded time were traceable to the National Bureau of Standards. All test data was recorded on strip chart recorders and a Model 133 CEC oscillograph.

The facilities and instrumentation employed in tests made at TRW Systems Group are described in Ref. 4.

F. Firing Procedures

During dynamic throttling tests, the signals shown in Figs. 8 and 9 (which had been prerecorded on tape) were used to activate the valve driver, which in turn operated the engine throttle valve. These signals are not necessarily representative of the kind that would normally be expected for a planetary lander engine duty cycle; rather, they were chosen to be of maximum utility to control-system engineers engaged in analysis of engine response. The "standard" square-wave and sinusoidal signals are most amenable to response analysis for system evaluation purposes.

As can be seen in Fig. 8, step inputs of widely varying amplitude were supplied. Starting at the 50% throttle position, steps of progressively larger amplitude, symmetric about the 50% position, were programmed. The initial step departed by about 2.5% from the 50% position, and successive steps progressively increased to 95%. The sinusoidal signal of Fig. 9 was somewhat more complex. After starting at the 50% position, the voltage was

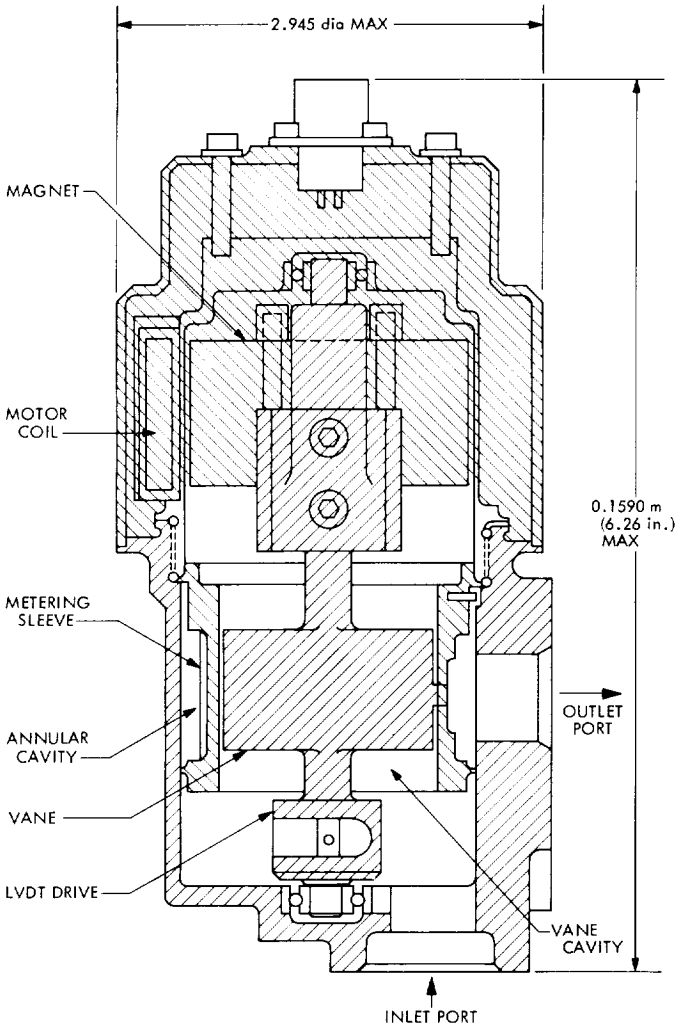

Fig. 6. Throttle valve 2

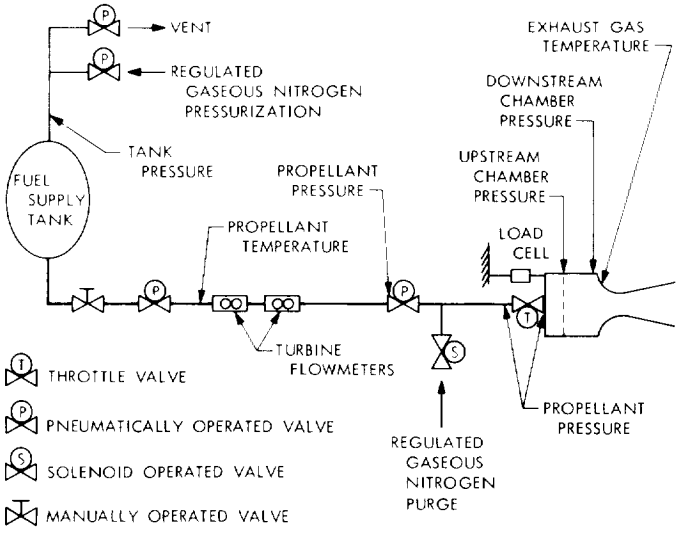

Fig. 7. Test setup schematic

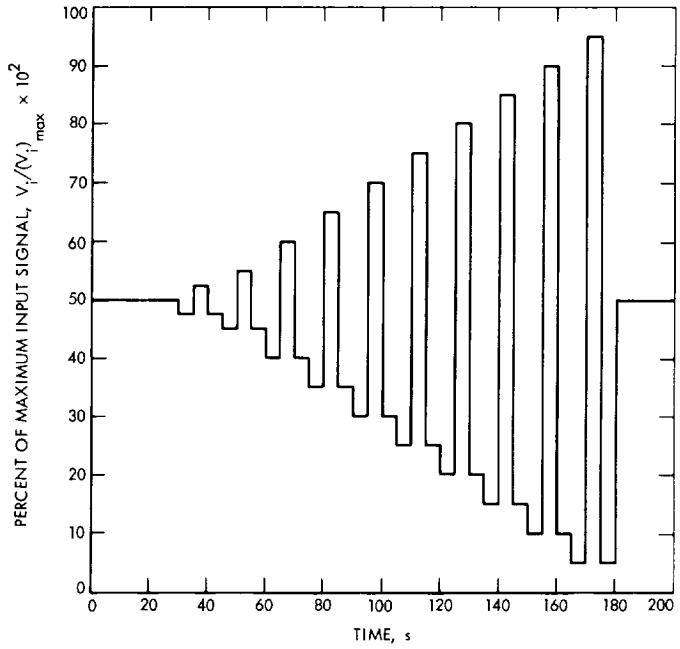

Fig. 8. Square-wave duty cycle for throttle valve tests

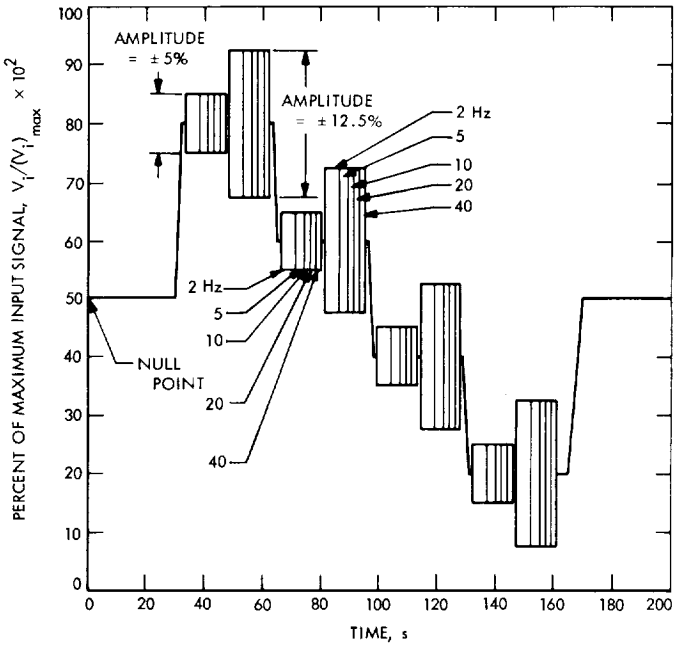

Fig. 9. Sinusoidal duty cycle for throttle valve tests

Table 3. Throttle valve characteristics

Parameter	Valve No. 1[a]	Valve No. 2[a]
Proof pressure	6.89 MN/m² (1000 psia)	5.12 MN/m² (800 psia)
Vented leakage	Not measurable at 3.45 MN/m² (500 psia for 15 min)	None
Weight	1.0 kg (2.2 lb_m)	1.2 kg (2.6 lb_m)
Position hysteresis	1.1% max	2.5%
Power	63 W at 28 Vdc	45.8 W at 28 Vdc
Step response wet	62 ms for 100%	8 to 45 ms for 90%
Overshoot	0%	35% for 90 to 100% step
Frequency response at 5 Hz	Amplitude ratio 0.98, phase angle −16 deg	Amplitude ratio 0.95, phase angle −16 deg
Maximum flow rate ΔP	0.469 MN/m² (68 psid)	0.228 MN/m² (33 psid)

[a]The valves are identified in Section III-D.

increased stepwise up to 80% of its maximum value. Then the system was throttled in a sinusoidal mode with amplitudes of ±5% and ±12.5% about the 80% reference position, at five sequential frequencies between 2 and 40 Hz. In a similar fashion, the system was progressively operated at throttle settings of 60, 40, and 20%.

IV. Experimental Results

A. Subscale Tests

1. Dynamic throttling. Dynamic throttling of two *Mariner* 1969 reactors was accomplished by means of a surplus *Surveyor* throttle valve (see Section III-A), driven by the taped input signals shown in Figs. 8 and 9. The steady-state c^* performance measured during each step shown in Fig. 8 is depicted in Fig. 10 as a function of mass flow rate. When compared to the equilibrium c^* of 1330 m/s (4370 ft/s), it can be seen that the engine approached equilibrium during each step. Thus, the performance was independent of flow rate except at flow rates below about 0.045 kg/s (0.1 lb_m/s). The significance of the correlation lines will be discussed in a subsequent section of this report.

The 90% response times corresponding to these step changes are shown in Figs. 11 and 12. These response times varied between 30 and 160 ms, depending on the change in pressure (size of throttle position change) and on whether an up-throttle (Fig. 11) or down-throttle (Fig. 12) step had occurred. For large pressure changes, both up- and down-throttle changes were similar; however, for smaller pressure changes the down-throttle steps were faster. During this exploratory subscale test series the response times were not always repeatable from one test to the next. In Figs. 11 and 12 the results of three different tests, each nominally at the same conditions, are shown. For both increasing and decreasing steps the response time varied about 60 ms over the three tests.

When the subscale engines were operated according to the sinusoidal duty cycle shown in Fig. 9, the chamber/valve combination response characteristics of Fig. 13 were obtained. In Fig. 13 the amplitude ratios and phase angles are shown in standard Bode plot format (Ref. 12) as a function of frequency for input signal amplitudes of ±5 and ±12.5%. Comparison of Figs. 13(a) and 13(b) reveals that the phase angle was independent of the impressed signal amplitude over a wide range of frequencies, but the amplitude ratio (in decibels) was dependent on the magnitude of the impressed amplitude. Between 2 and 40 Hz, the phase angle varied between −30 and −430 deg respectively for both amplitudes. The corresponding amplitude ratios at ±5% impressed amplitude ranged from +7 to −11 dB, while at ±12.5% they ranged from +5 to −15 dB.

Note that because the *Surveyor* throttle valve had no position indicator, the response times reported above are for the thrust chamber/valve combination. It is not possible to discriminate between the contributions to this response of the chamber and valve.

2. Heat sterilization. Two *Mariner* 1969 reactors were used for this test series. In the first test on the two reactors, baseline c^* performances of 1330 m/s (4360 ft/s) and 1320 m/s (4320 ft/s) respectively were established. The reactor ignition characteristics are summarized in Table 4. Holding the SN 008 reactor as a control, SN 005 was heat sterilized. A subsequent firing determined that sterilization had little effect on characteristic velocity, but the ignition delay increased from 98 to 159 ms, the peak pressure increased 1.44 MN/m² (209 psi) and the pressure rise time increased from 67 to 85 ms.

3. Long-duration steady-state firings. Two tests were conducted with *Mariner* 1969 reactors to investigate the possible effects of long-duration firings. During this test series chilled hydrazine at 280 K (45°F) was used to simulate thermal conditions on certain contemplated outer planet missions. Both tests were conducted for a period of 1000 seconds. For the most part, engine performance remained nominal for the entire duration of

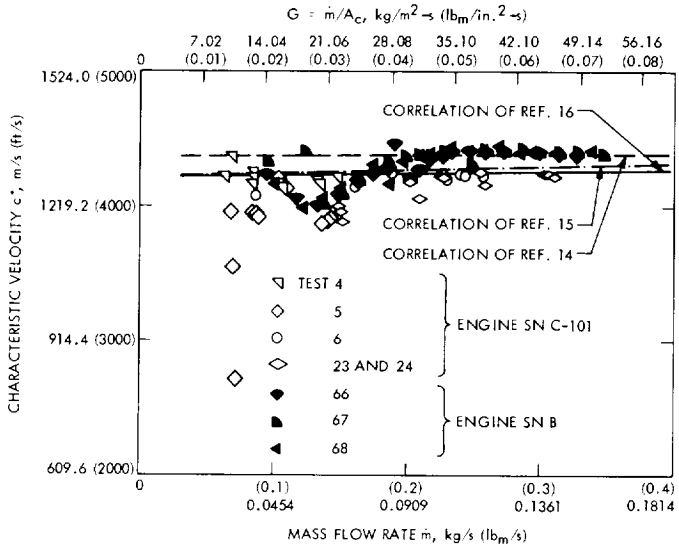

Fig. 10. Steady-state performance of *Mariner* Mars 1969 engine as a function of flow rate

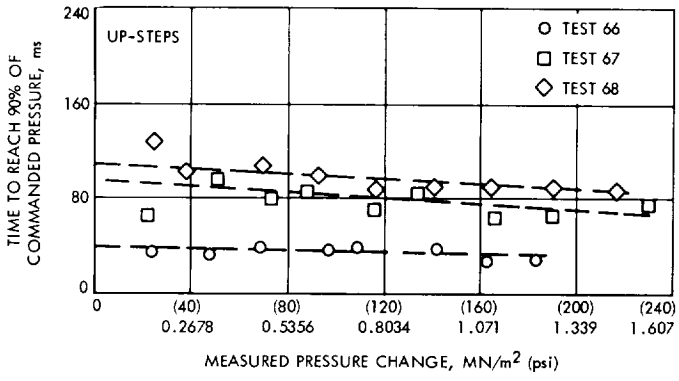

Fig. 11. Response of *Mariner* Mars 1969 engine to pressure increase

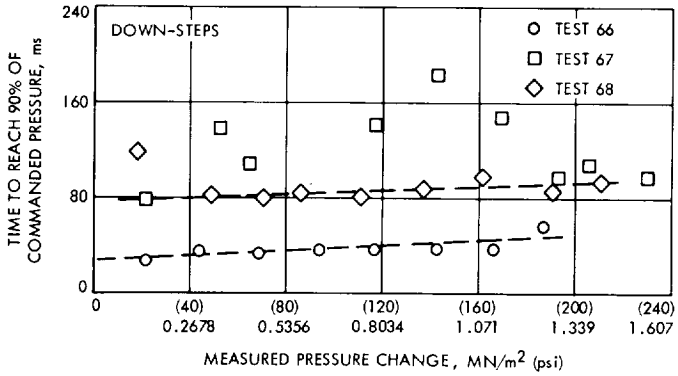

Fig. 12. Response of *Mariner* Mars 1969 engine to pressure decrease

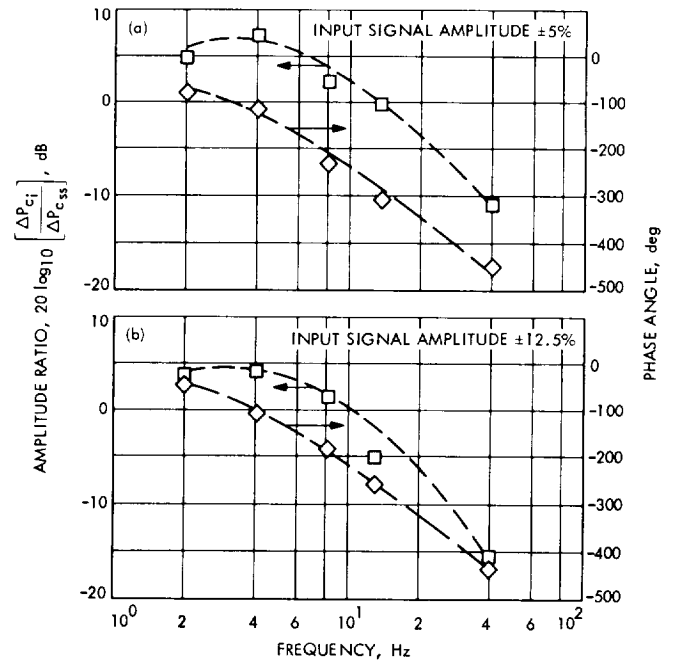

Fig. 13. Amplitude ratio and phase lag vs frequency input signal for *Mariner* Mars 1969 engines: (a) amplitude ±5%, (b) amplitude ±12.5%

Table 4. Summary of heat sterilization experimental results

Engine No.	P_c (avg)		Mass flow rate m		Characteristic velocity c^*		Roughness index $\frac{\Delta P_c}{2P_c}$	Ignition delay, ms	Peak pressure		Pressure rise time, ms
	MN/m²	psia	kg/s	lb_m/s	m/s	ft/s			MN/m²	psia	
SN 005	1.426	206.8	0.106	0.234	1328.9	4360	2.4	98	1.689	245	67
SN 008	1.293	187.6	0.097	0.214	1316.7	4320	2.0	100	1.420	206	50
SN 008	1.309	189.8	0.098	0.216	1313.7	4310	1.9	129	1.406	204	60
SN 005[a]	1.426	206.9	0.106	0.234	1331.9	4370	2.0	159	3.130	454	85

[a]After sterilization

both tests; however, one anomaly did occur in the first test. After steady-state operation had been established for 225 s, the engine pressure drop increased from 0.186 MN/m² (27 psia) to 0.702 MN/m² (102 psia), and only partly recovered 125 s later. Around the same time, the characteristic velocity fell 30.48 m/s (100 ft/s). Figure 14 portrays these effects. During this test the chamber pressure roughness increased from ±0.0344 MN/m² (5 psi) to ±0.414 MN/m² (60 psi) in the first 400 s, but decreased to ±0.138 MN/m² (20 psi) after 600 s. During the test it was possible to visually observe external heat patterns on the engine, which may be regarded as a rough indication of the location of the reaction zone. One particular incandescent zone started near the injector face, migrated into the bed, and then returned to the vicinity of the injector face. This same effect can be identified in Fig. 14 because thermocouples in the bed indicated gross temperature variations as the reaction zone receded into the bed and returned to the region of the injector face.

The second test showed no such behavior, but the engine roughness started at ±0.0344 MN/m² (5 psi) and steadily increased to ±0.138 MN/m² (20 psi) during the test. The pressure drop, chamber temperature, and characteristic velocity continually decreased throughout the test, as shown in Fig. 15.

B. Full-Scale Tests

Tests on the full-scale engines and throttle valves 1 and 2 were conducted at TRW and JPL. All valve characterization tests were conducted at TRW.

1. Valve characterization. Two types of tests were conducted on valve 1[4]. The first was a flow calibration, the results of which are presented in Fig. 16. The valve was calibrated from 0.174 kg/s (0.383 lb_m/s) to 1.135 kg/s (2.5 lb/s). The feedback (output) voltage was nearly linear with flow rate but not with pressure drop. The pressure drop ranged from 0.4 MN/m² (58 psi) at maximum flow to over 2.31 MN/m² (335 psi) at the low flow rate. Note that, as with most throttle valves, pressure drop is inversely proportional to flow rate.

The second category of tests on this valve determined its dynamic response characteristics. These test results are included in Table 3. The valve's response to an impressed sinusoidal signal of 5 Hz was characterized by a phase angle of −16 deg and an amplitude ratio of 0.98 dB. The step response was 62 ms for a 100% change.

A flow calibration of valve 2 is presented in Fig. 17. As with valve 1, the flow rate and pressure drop are inversely related. The flow calibrations were made from 0.045 kg/s (0.1 lb_m/s) to 0.907 kg/s (2.0 lb_m/s), with the corresponding pressure drops being 2.54 MN/m² (368 psi) and 0.34 MN/m² (50 psi). Feedback voltage was slightly nonlinear with both parameters.

Response characteristics of this valve are also shown in Table 3. Its frequence response (−16 deg phase angle and 0.95 dB amplitude ratio) was very similar to that of the other valve. An examination of Table 3 reveals that, compared with valve 1, this valve was slightly heavier, had a greater degree of hysteresis, and a significant "overshoot."[5] However, the step response[6] between 8 and 45 ms was shorter than that of valve 1.

[4]The valves are identified in Section III-D.

[5]Overshoot is the degree (percentage) to which the valve position will exceed the desired position on initial movement. This is followed by damped oscillations which converge on the final valve position.

[6]Step response is the time required to reach the final valve position when the valve is subjected to a step input signal.

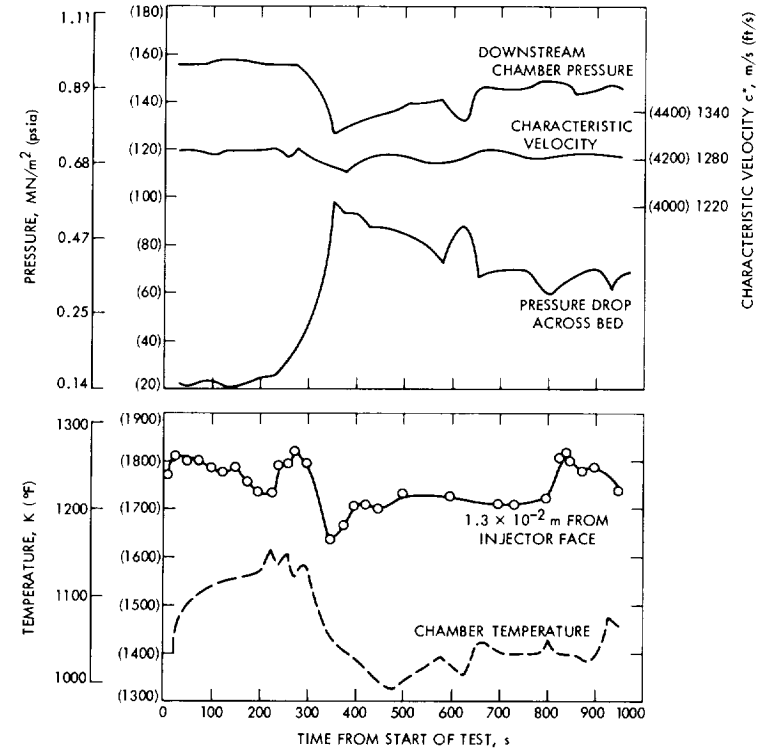

Fig. 14. First 1000-s firing of *Mariner* Mars 1969 engine

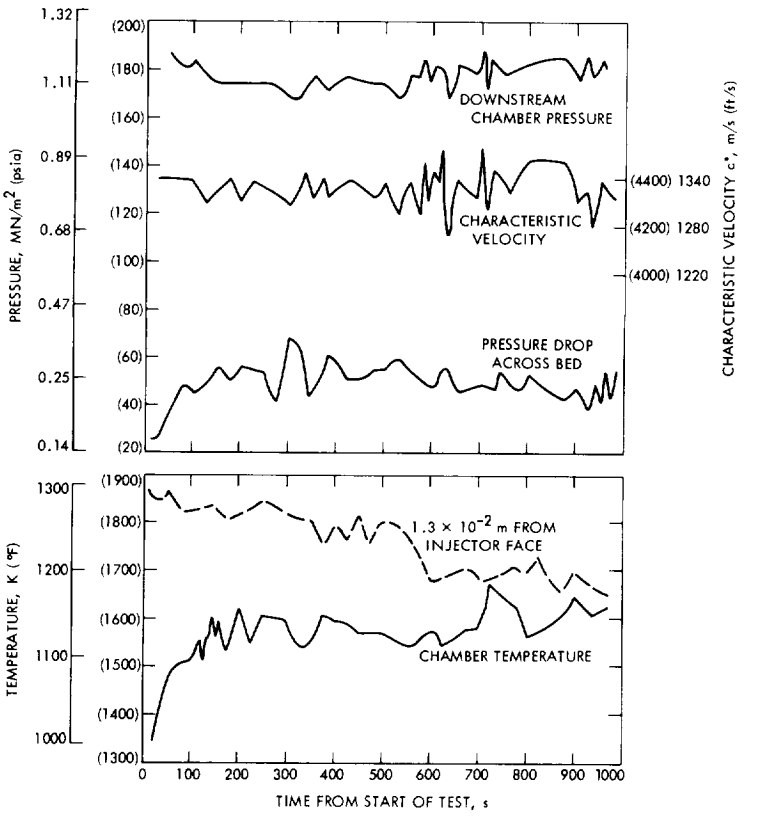

Fig. 15. Second 1000-s firing of *Mariner* Mars 1969 engine

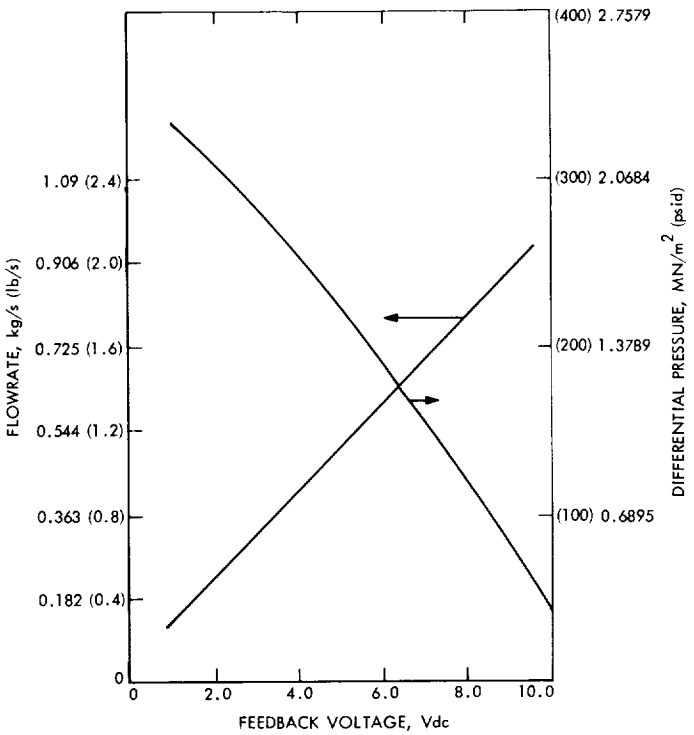

Fig. 16. Flow calibration for throttle valve 1

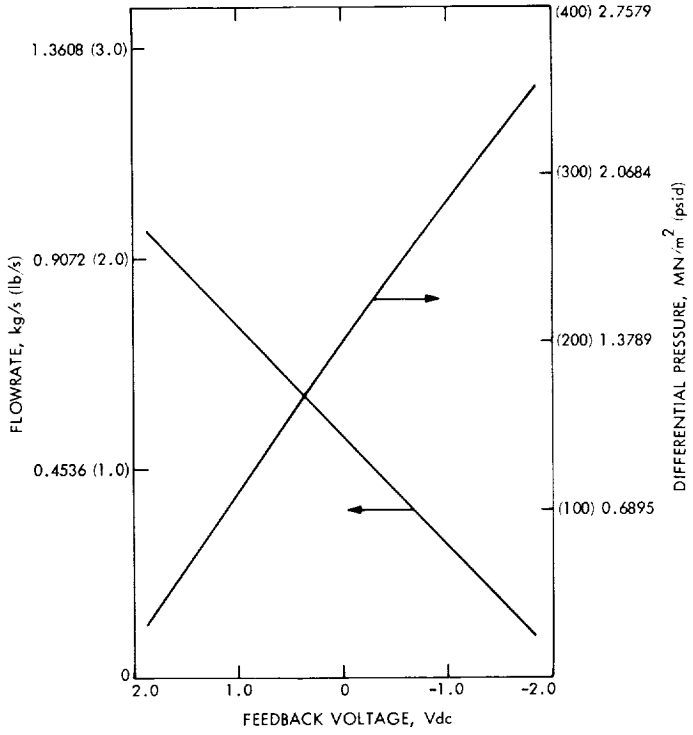

Fig. 17. Flow calibration for throttle valve 2

Two problems were encountered with valve 2. At the null point (half open position), it exhibited a 50-Hz oscillation or "flutter," about its set position. This problem was believed to be associated with improper matching of the valve and drive amplifier. The motion was critically damped during flow, and could be permanently minimized by reducing the amplifier gain or adding electronic compensation.

The second problem resulted from this valve's narrow force margin[7] and the apparently unbalanced dynamic forces on opposite sides of the vane (see Fig. 6). At high flow rates and inlet pressure (2.07 MN/m^2, 300 psia), the unbalanced forces acted to close the valve, and the available force margin was insufficient to counteract this effect. Thus, at design inlet pressure, this valve always shut itself off at or near full-thrust flow rates. Because of these functional anomalies, valve 2 was excluded from further testing.

2. Heavyweight engine firings. All firings of the heavyweight engine were conducted in test cell "J" at JPL's Pasadena facility with throttle valve 1.

[7]Force margin is the difference between the force required to produce a given valve motion and that available to do so.

Steady-state characteristic velocity (uncorrected for viscous, expansion, or other losses) is shown in Fig. 18 as a function of mass flowrate and catalyst bed loading. The data shown was taken during steady-state intervals of step-throttling firings. Characteristic velocity remained constant at a mean value of 1295 m/s (4250 ft/s) at all flow rates above 0.2 kg/s (0.44 lb_m/s). The significance of the correlation lines is discussed in a subsequent section of this report.

The characteristic velocity to be expected from theoretical considerations depends on the degree of ammonia dissociation. Chemical analysis of the gaseous exhaust products indicated that 85% of the ammonia was dissociated, while measurements of gas temperature (1103 K, 1525°F) corresponded to a decomposition fraction of only 71%. Based on these values of ammonia dissociation, the uncorrected engine characteristic velocity efficiency was close to 100%. If one assumes, as a lower limiting case, an ammonia decomposition equal to the optimum value of 25 to 30%, the c^* efficiency is still 96.5%.

When subjected to the square-wave input signal of Fig. 8, the thruster/valve combination response time varied between 40 and 80 ms, depending on the size of the steps.

These response characteristics are shown in Fig. 19 as a function of the step change in chamber pressure. In contrast to the *Mariner* 1969 reactor used in the subscale throttle tests, there was little hysteresis between increasing and decreasing pressure steps, and the response times were very reproducible from one test to the next.

Typical sinusoidal (Fig. 9) response characteristics are shown in Fig. 20 for the ±5% amplitude signal and in Fig. 21 for the ±12.5% amplitude signal. For a frequency of 5 Hz with a ±12.5% amplitude the phase angle remained near −80 deg. Considerable difficulties were encountered in determining the amplitude ratio. Data scatter both during a test and from one test to the next made it difficult to correlate this data.

At 5 Hz for the ±12.5% amplitude signal, the amplitude ratio ranged from +3 to −3 dB. At 5 Hz for the ±5% variation, the phase angle and amplitude ratio were −70 deg and +1.3 to −1.3 dB, respectively. This indicates significant increases in these response parameters as a result of increased signal amplitude. Variations in these two parameters were not affected by throttle setting within the degree of precision of this experiment.

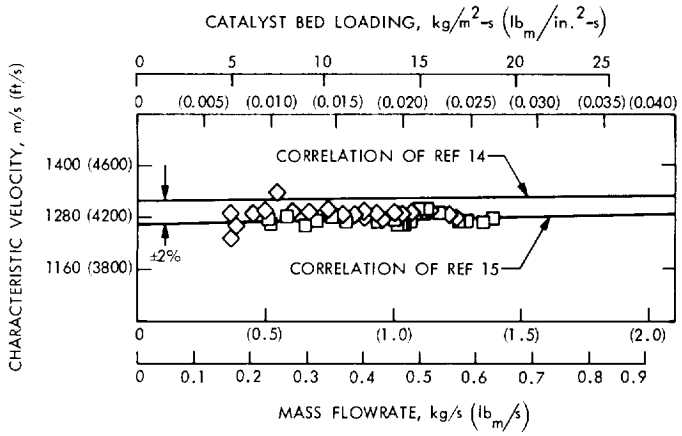

Fig. 18. Steady-state characteristic velocity vs mass flowrate for heavyweight engine

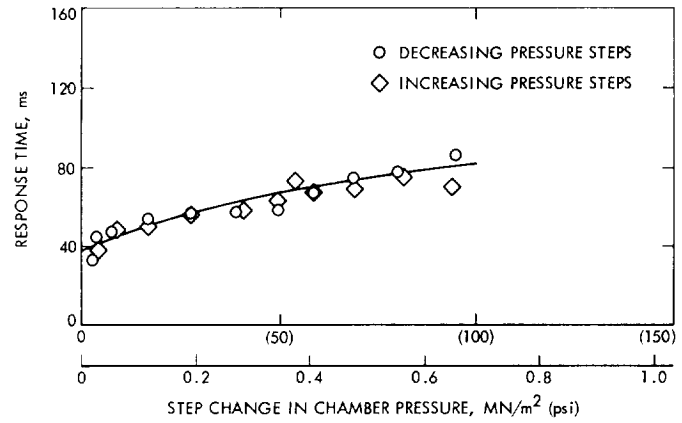

Fig. 19. Response of heavyweight engine to square-wave input

This engine ran smoothly, the peak-to-peak chamber pressure roughness being at all times less than 1% of the mean chamber pressure.

3. Lightweight engine firings. Following fabrication, the lightweight engine was fired at TRW with throttle valve 1 to characterize its performance prior to heat sterilization. The sterilization cycle was relaxed from that used on the subscale tests (see Sec. IV-A-2) to three cycles of 35 h exposure to dry nitrogen at 408 K (276°F). A comparison of the engine performance before and after sterilization indicated no change in c^* performance (Ref. 4). During three 330 ms firings of the engine (as originally configured) at 40, 100, and 70% throttle, a c^* performance of 1332 m/s (4370 ft/s) was measured. The chamber pressure roughness averaged about ±34%. Following the modification in the catalyst bed geometry described in Section III-C, the c^* performance was 1340 m/s (4400 ft/s) but the roughness had been reduced to ±11%. The engine was then characterized, and the test results are shown in Table 5.

Table 5. Lightweight engine performance demonstration test results[a]

Function	Demonstrated
Thrust	Not measured
Throttle ratio	5:1
Overexpansion	Not measured
Vacuum specific impulse	2158 Ns/kg (220 lb_f-s/lb_m) to 2256 Ns/kg (230 lb_f-s/lb_m)[b]
Durability	>174 s (testing incomplete)
Sterilization	3 cycles of 35 h @ 408.1 K (275°F)
Vibration	Not tested
90% step response (engine)	85 ms (80% step)
Step response (valve)	67 ms (80% step)
Amplitude ratio (engine)	−0.44, @ 60 ±25% and 5 Hz
Phase angle (engine)	−36 deg @ 60 ±25% and 5 Hz
Overshoot (engine)	<10%

[a]Firings performed by TRW Systems Group, Redondo Beach, California.
[b]Based on c* results at sea level.

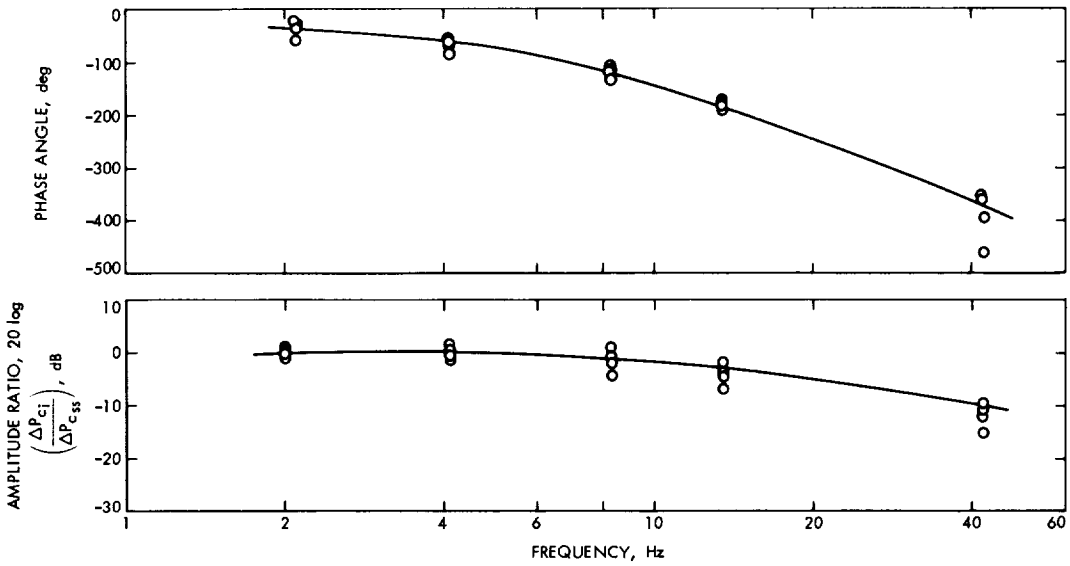

Fig. 20. Phase angle and amplitude ratio vs frequency for heavyweight engine (±5% amplitude)

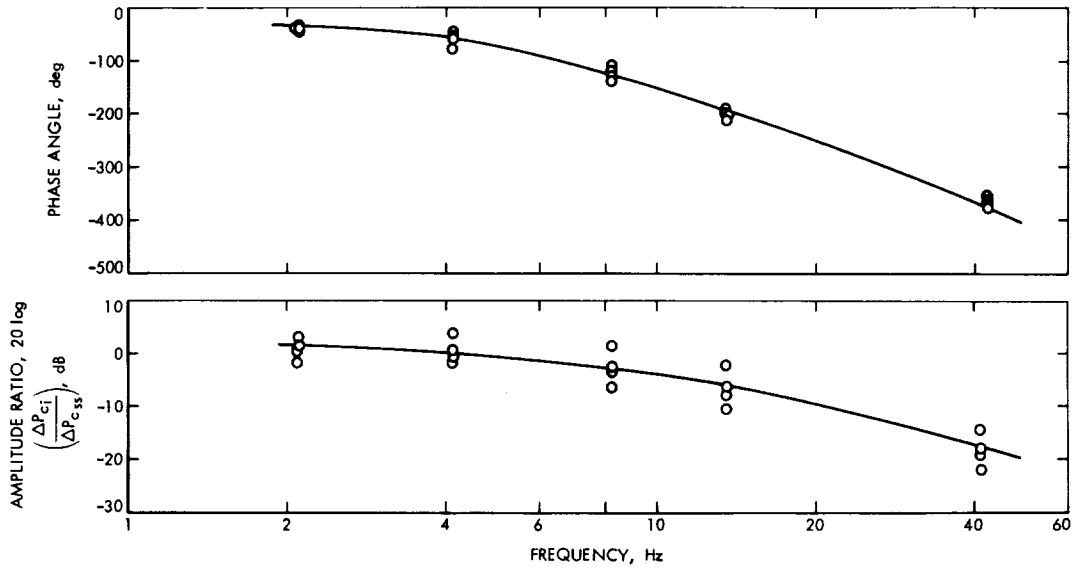

Fig. 21. Phase angle and amplitude ratio vs frequency for heavyweight engine (±12.5% amplitude)

From Table 5 it can be seen that the vacuum specific impulse decreased only from 2.25×10^3 N-s/kg (230 lb_f-s/lb_m) to 2.16×10^3 N-s/kg (220 lb_f-s/lb_m) while mass flow was throttled down over a range of 5 to 1. These values of specific impulse were calculated from characteristic velocity measurements. When subjected to an 80% step input, the engine response time was 85 ms. For a 5-Hz sinusoidal input at a 60 ±25% throttle position, the amplitude ratio and phase angle were −0.44 and −36 deg, respectively. Further details of these tests may be found in Ref. 4.

Additional firings of the lightweight thruster/valve 1 combination were conducted at test cell "J" at JPL in Pasadena. It was found that the c^* performance of this engine was 1330 m/s (4370 ft/s) and nearly independent of propellant flow rate above about 0.23 kg/s (0.5 lb_m/s). Figure 22 depicts these results as a function of mass flow rate. Step response of this engine varied between 25 and 80 ms as shown in Fig. 23. As can be seen, the engine responded more quickly to increasing pressure steps. This difference between response for increasing and decreasing steps was opposite to that observed in the subscale throttle tests. The increasing pressure response times varied from 45 to 53 ms for chamber pressure changes of 0.31 MN/m² (45 psia) to 0.83 MN/m² (120 psia), while the decreasing pressure response times varied from 25 to 80 ms for chamber pressure changes from 0.24 MN/m² (35 psia) to 0.79 MN/m² (115 psia).

Sinusoidal response of this engine to ±5 and ±12.5% signal amplitude can be seen in Figs. 24 and 25. As with the heavyweight engine, reasonable reproducibility could be obtained for the phase angle; however, the amplitude ratios were somewhat more scattered. At 5 Hz and ±12.5% amplitude, the phase angle was about −70 deg while the amplitude ratio ranged from +1 to −1 dB. Again, as with the other engine, these parameters were not sensitive to the input pressure within the limits of precision of this test.

Peak-to-peak chamber pressure roughness on this engine was approximately ±8% of mean chamber pressure. This compounded the problem of determining reproducible amplitude ratios. Above 20 Hz it was impossible to discriminate between "signal" and "noise" in the data.

Several tests were conducted to determine the effects of amplifier gain on system dynamic response. With sinusoidal inputs of ±12.5% amplitude, the results depicted

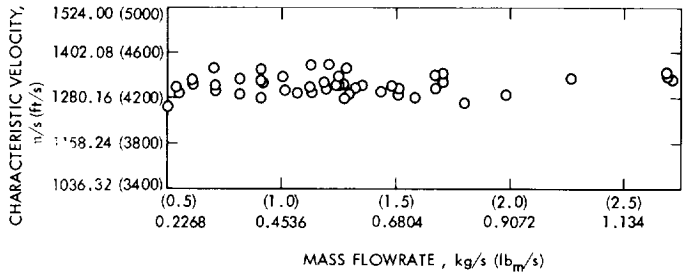

Fig. 22. Steady-state characteristic velocity vs mass flowrate for lightweight engine

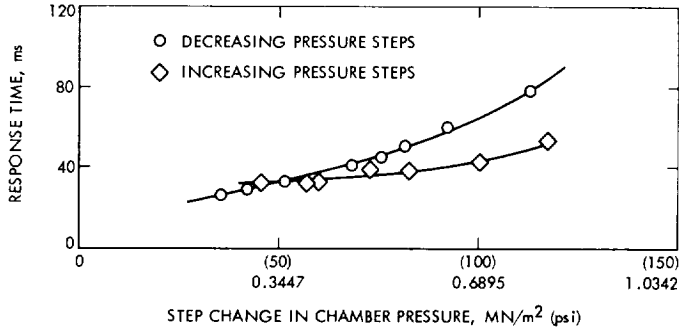

Fig. 23. Response of lightweight engine to square-wave input (amplifier gain = 100)

in Fig. 26 were obtained. As can be seen, higher amplifier gain increased the thruster/valve amplitude ratio but had little effect on phase angle. At 5 Hz with the amplifier gain set at 75, the amplitude ratio and phase angle were about −1 dB and −70 deg.

The response of the lightweight engine to a square-wave input at an amplifier gain of 75 is plotted in Fig. 27. Comparison of this response with that shown in Fig. 23 for a gain of 100 indicates a slower response time at the lower gain. However, differences between increasing and decreasing steps are hard to discern because of data scatter in both cases.

Using a measured steady-state gas chamber temperature of 1206 K (1708°F), it was determined that the degree of ammonia decomposition was at least 58%.

During the course of the test program, over 1500 s of firing time was accumulated on the lightweight engine.

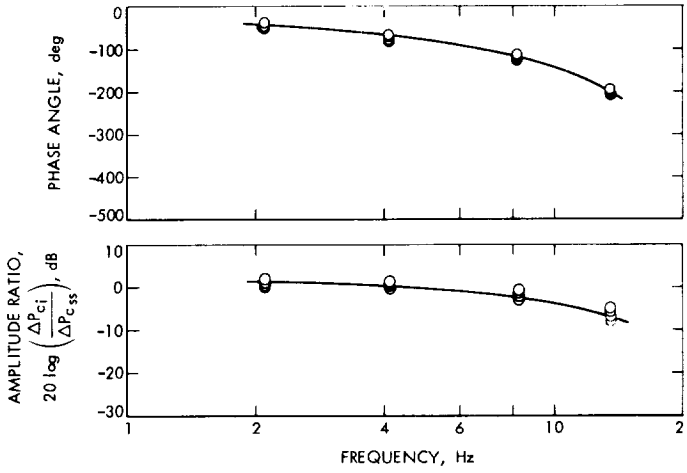

Fig. 24. Phase angle and amplitude ratio vs frequency for lightweight engine (±5% amplitude)

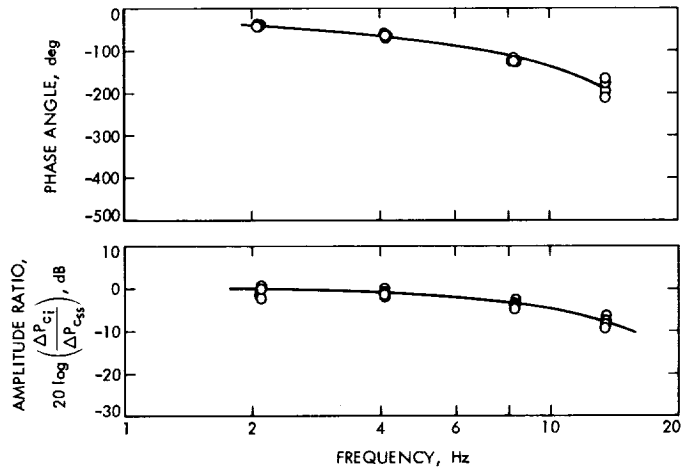

Fig. 25. Phase angle and amplitude ratio vs frequency for lightweight engine (±12.5% amplitude)

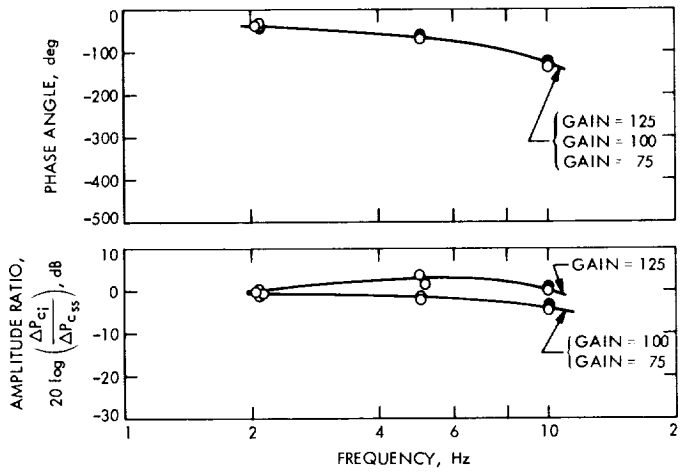

Fig. 26. Phase angle and amplitude ratio vs frequency for amplifier gains of 75 and 125; lightweight engine (±12.5% amplitude)

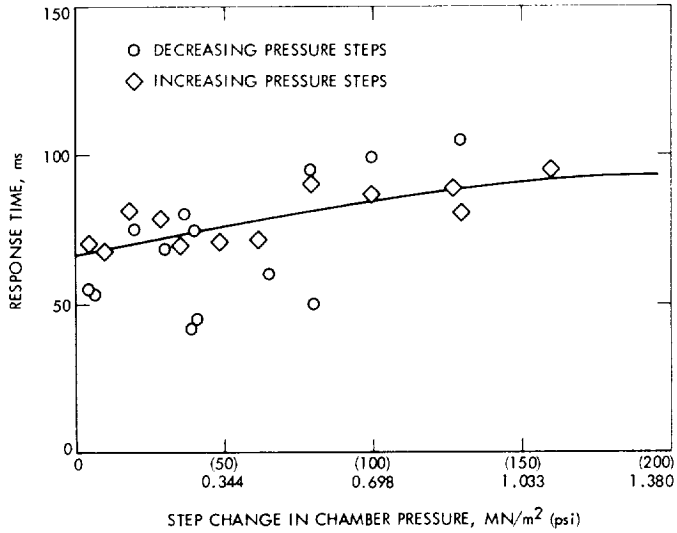

Fig. 27. Response of lightweight engine to square-wave input (amplifier gain = 75)

Upon final examination, it was observed that some catalyst "fines" had infiltrated the retainer screens; however, no significant effect on characteristic velocity performance or engine roughness was seen.

V. Discussion of Results

A. Subscale Tests

1. Dynamic throttling. No conditions of dynamic instability were observed during the subscale testing. The c^* performance measured during dynamic throttling was comparable to that measured during steady state, 1330 m/s (4370 ft/s).

Included on Fig. 10 are the performance predictions derived from Refs. 14, 15, and 16. Given the reactor geometry, fuel flow rate, chamber pressure, and the catalyst particle size and distribution, these references predict the composition of the gases leaving the catalyst bed. For monopropellant hydrazine, the theoretical characteristic velocity is a unique function of the gas composition. Thus, for a given reactor, c^* as a function of mass flow rate can be predicted. Experimental c^*s are generally a large fraction of the theoretical values since catalytic reactors are not nearly as susceptible to mixing and atomization losses as are bipropellant injectors. However, while the predictions from Refs. 14, 15, and 16 are in reasonable agreement among themselves[5], none predict the observed performance degradation at the lower flow rates evident in Fig. 10.

Since all three referenced correlations are based on data taken at bed loadings as low as 7.04 kg/m^2-s (0.01 lb$_m$/in.^{2}-s) it is concluded that the present performance degradation, as well as the erratic nature of the data at such low flow rates, results from a source other than excessive ammonia dissociation. Although it is known that propellant atomization is less important for hydrazine catalytic reactors than for a bipropellant engine, it is hypothesized that this may be the source.

Two of the step response tests on the *Mariner* 1969 reactor met the *Viking* lander requirements of 95 ms for any 90% step. As shown in Fig. 11, the response time during a third test (test 68) did not meet those requirements. Variations of this kind between firings and between up- and down-throttle steps would probably not be acceptable for a flight lander engine application such as *Viking*. It should be remembered, however, that the primary objective of this set of subscale experiments was to gain throttling system experience in preparation for evaluation of the high-thrust reactors.

When operated to the sinusoidal duty cycle, the dynamic response characteristics of this reactor were again such that they would probably not meet the requirements of a typical flight application, such as *Viking*. For example, for an input signal with a frequency of 5 Hz and an amplitude of ±25% about a throttle setting of 60%, *Viking* requires an amplitude ratio of greater than −2 dB with a phase angle greater than −52 deg. Under these same conditions the *Mariner* 1969 thruster amplitude ratio and phase angle were 4 dB and −120 deg. The choice of *Viking* lander requirements as a standard against which to compare the measured dynamic response characteristics of these and the larger reactors was, of course, rather arbitrary.

2. Heat sterilization. As previously reported, heat sterilization had only minor effects on reactor performance. This was not surprising, since the catalyst normally operates at temperatures far in excess of those required for sterilization. The variations in start transient (ignition delay, pressure rise time, and peak overshoot) most likely resulted from a temporary reduction in activity of the Shell 405 catalyst. Nitrogen molecules from the sterilization environment may have been physically adsorbed on part of the active sites until driven off by the heat of the incipient reaction. This may have allowed an accumulation of partially decomposed fuel in the chamber prior to ignition, which would explain the surge in chamber pressure before equilibrium was established. Once the reaction started, the catalyst activity would have been restored and normal steady-state performance achieved. Such a temporary inactivation would not be expected after long-term exposure of a reactor to the space environment, because any molecules adsorbed during the sterilization cycle would have long since desorbed to space vacuum.

3. Long-duration steady-state firings. No completely satisfying explanation of the anomalous temperature and pressure fluctuations encountered during the first firing can be offered. However, based on the observed incandescent zone migration, it may be postulated that after exposure to cold incoming propellant for some time, the

[5]Note that Ref. 14, strictly speaking, is not applicable to the Shell 405 catalyst used in these tests. Comparison between the correlation of Ref. 14 and the present data was attempted, however, because of the lack of agreement between experiment and the theories of Refs. 15 and 16 at low flow rates. As expected, Ref. 14 predicts a higher c^*, but again the dependence on m is slight and of the same order of magnitude as in the other two works.

catalyst activity near the injector face decreased and the reaction zone migrated further into the bed. This reduction in effective bed length could have reduced the ammonia dissociation and therefore the volumetric flow; however, it would have increased the stagnation temperature, so the resulting change in pressure drop would have been small, as was observed. When the reaction zone had receded a sufficient distance into the bed, the vaporized unreacted propellant would have had to diffuse through the catalyst void volume. Since, because of density differences, the pressure drop of vaporized hydrazine is greater than that of the decomposition gases at constant mass flow rate, it is not surprising that the overall reactor pressure drop increased. When, for some as yet unexplained reason, the flame front returned to the vicinity of the injector face, the pressure drop began to decrease.

It may be speculated that the anomalous behavior observed here may have been incipient "washout." Washout is a phenomenon, observed by some industrial suppliers of Shell 405 catalytic hydrazine reactors, characterized by a drastic decrease in chamber pressure and a nearly total cessation of hydrazine decomposition. It has most frequently been observed in firings of long duration with cold propellant, in reactors with relatively low catalyst specific surface area and high superficial mass velocity ("bed loading"). The authors share the view, originally suggested by Sangiovanni and Kesten (Ref. 13), that a likely explanation of this phenomenon is preferential adsorption of hydrogen and ammonia molecules on active catalyst sites under the conditions of high pressure and low temperature prevailing in the upstream regions of the bed. This process would tend to proceed through the bed until enough active sites had been blocked that the decomposition reaction could no longer be sustained.

If the behavior observed in the present experiment were indeed attributable to incipient washout, it would appear that the *Mariner* 1969 reactor was able to spontaneously recover. Such recovery has been observed by other investigators.[9] However, it cannot be assumed that the same phenomenon would not have occurred again, perhaps with more aggravated symptoms, had the reactor been fired for still longer durations. The absence of these anomalies from the second firing has yet to be explained.

[9]R. J. Rollbuhler, NASA Lewis Research Center, Cleveland, Ohio, private communication.

B. Full-Scale Tests

1. Characterization of throttle valve 1. The valve performance met the specifications established for it during preliminary design of the throttleable thruster system. It may be instructive to compare its delivered performance with that required by a typical planetary lander application. The *Viking* lander, for example, required a sinusoidal amplitude ratio and phase angle at 5 Hz equal to or less negative than −0.98 dB and −16 deg, respectively, and this valve delivered exactly those values. However, its step response of 62 ms was well within the 80-ms limits required by *Viking*. This valve functioned very well during the limited research testing conducted with it. It was observed, however, that its response characteristics were quite sensitive to valve drive amplifier settings.

2. Heavyweight engine. The characteristic velocity performance plotted in Fig. 18 is seen to remain nearly constant over the throttle range evaluated, which was about 4.33:1. This is in contrast to the results of the subscale engine throttle tests discussed earlier. Whatever the cause of the performance drop of the *Mariner* 1969 reactor, the results with this larger reactor show that this effect is *not* a universal characteristic of catalytic hydrazine reactors, and that a significant performance loss is not necessarily an inevitable result of throttling.

If it is assumed that the measured characteristic velocities of Fig. 18 correspond to an energy release efficiency of 100%, then the apparent ammonia dissociation level is slightly over 60%. The existing correlations of characteristic velocity with bed loading (or mass flow rate) are strictly valid only for reactors employing either 100% Shell 405 or 100% nonspontaneous catalyst. The present reactor, of course, contained both. Thus, it is somewhat difficult to judge the validity of the assumed 100% energy release efficiency. Included in Fig. 18 are lines representing two predictions (Refs. 14 and 15), one for each type of catalyst bed. The large majority of all the measured performance data falls between the two predictions, as would be expected. Thus, the heavyweight reactor performed well, and there apparently were no significant losses.

Roughness is another criterion of importance for judging reactor operation. In this area, the reactor performed exceptionally well. The chamber pressure variations during steady-state operation were less than 1% of mean chamber pressure. There was concern after the initial tests that the 0.15 to 0.3 m (6 to 12 in.) of 6.35-mm

(¼-in.) tubing used to connect the pressure transducers to the thrust chamber might be severely distorting and damping the pressure signal. The gauges were then close-coupled to the engine with no change in the signal shape. A high-response (10,000-Hz) gauge was also employed in several tests, again verifying the excellent roughness characteristics.

Although *Viking* allows an engine roughness of ±10%, it is desirable to have a smooth-running engine. From this standpoint the less than 1% roughness of the heavyweight engine far exceeded the requirement. It was felt that either or both the showerhead injector and HA3 catalyst were responsible for this smooth operation.

Dynamic throttling is another technology area of major concern. When operated to the step input duty cycle of Fig. 8, the response times of the heavyweight engine varied between 40 and 80 ms. The longer times occurred with the larger pressure changes. These response times, of course, can only be judged against some arbitrary standard, which in this case was 75 ms, the *Viking* lander requirement at the time of inception of this work. The engine met the 75-ms response time only for small step sizes. The reason for this may well be inherent in the large propellant manifolding required by the showerhead-type injector.

In sinusoidal operation with ±12.5% amplitude, the heavyweight engine met the *Viking* amplitude ratio requirements at all frequencies, but its phase angle was excessive above 5 Hz. A comparison between ±5 and ±12.5% amplitude revealed that the phase angles for any other frequency were similar; however, the amplitude ratio for ±5% amplitude was less.

3. Lightweight engine. The higher c^* performance of the lightweight engine (about 1334 m/sec) compared to the heavyweight engine (1295 m/s) may be attributed to its higher bed loading and its reduced quantity of catalyst, both of which may have resulted in a lower degree of ammonia dissociation. A high degree of confidence was assigned to this value of c^* for the lightweight engine, since independent measurements made at TRW Systems (1340 m/s) and JPL (1330 m/s) were within 1% of one another.

The variations between increasing thrust and decreasing thrust step response times (30 ms at 45 psid to 50 ms at 115 psid as opposed to 30 ms at 45 psid to 80 ms at 115 psid) were most likely caused by the nonlinear characteristics of the valve. Dynamic forces caused by flow through the valve tend to close it. Consequently, the valve response time is slower if the pintle motion is against these forces rather than with them. Despite this hysteresis, the engine system response was better than the 80 ms required for the *Viking* lander application.

The initial chamber pressure roughness (±34%) was attributed to two causes: (1) the void volume below the injector face, and (2) a postulated nonuniform flow distribution through the catalyst bed. In the first case, the gas cavity so formed was probably very unstable and could have allowed the accumulation of liquid drops on the injector screen. Sporadic ignition of these droplets is one likely cause of the observed pressure fluctuations. The nonuniform flow pattern can be explained in terms of the difference in pressure drop through the two concentric cylindrical catalyst beds. Since beds of coarse catalyst particles have low pressure drops compared to beds of fine particles, it is not surprising that most of the flow would follow a path through the coarse bed. Rough chamber pressure is a characteristic of large-particle catalyst beds. After the catalyst bed geometry was modified from one of concentric cylinders to one of concentric hemispheres (layered beds), the fuel flowed to a greater extent through both beds. Thus, it was possible to reduce chamber pressure roughness to the final measured value of ±8%. This residual ±8% roughness is most likely a result of the large void volume below the injector face.

As stated earlier, the amplifier gain had little effect on system phase lag, but did exert a strong influence on the amplitude ratio. Further, in the case of valve 2, the 50-Hz oscillations were reduced through the use of a lower amplifier gain. Consequently, amplifier gain would seem to emerge as a significant system parameter for throttleable thruster systems.

Although it is difficult to generalize from the limited step response data available, it appears that the engine response time decreases with decreasing amplifier gain and, therefore, the variations between response during increasing and decreasing thrust steps are reduced at the lower gains. A comparison of step response times for amplifier gains of 100 and 75 indicates that the step response times for the two cases approach one another as the pressure change increases.

The generation of fines after 1500 s of operation is typical of the kinds of catalyst used and so was not surprising. It is possible that improved catalyst retention methods could minimize this effect somewhat, as indi-

cated by related experience at JPL. Rough reactor operation also tends to generate fines, as it causes loosening of the catalyst bed and permits abrasion of one particle against another.

VI. Advanced Lightweight Engine Design

Based on the results of this work, an advanced lightweight engine was designed, incorporating the best features of the two full-scale engines evaluated, as well as several new design features. This design is shown schematically in Fig. 28, and its design parameters are summarized in Table 6. It was considered to be representative of the state of the art of high-thrust throttleable hydrazine engines at the time of completion of the present work.

Using an elliptical chamber geometry with L605 material, an estimated loaded engine weight of 4.7 kg (10.4 lb_m) was achieved. Since an operational life in excess of 1500 s was attained with the previous full-scale lightweight engine, engine life was not given special attention in the design of this advanced version. However, the catalyst bed loading was held to a maximum of 77 kg/m^2-s (0.11 $lb_m/in.^2$-s). The engine was designed for use with a throttle valve similar to those evaluated and had an inlet fitting that would accommodate either. This engine had a two-layered catalyst bed. The upper bed consisted of 7.62 mm (0.3 in.) of 14-18 mesh Shell 405 catalyst and the lower of 37.1 mm (1.46 in.) of 3.2-mm (⅛-in.) HA3 catalyst pellets. The HA3 catalyst was selected for the lower bed because experience has shown that it contributes to smooth reactor operation. The catalyst was held in place with Haynes 25 screens backed by Haynes 25 retaining plates. Based on the relative smoothness of combustion exhibited by the showerhead injector in the heavyweight engine, a showerhead pattern was chosen for the advanced lightweight design, as well. An injector manifold incorporating both peripheral and central feed was designed to provide adequate cooling near the peripheral injector-chamber weld joint. It was felt that, in the absence of peripheral feed, it was possible for fuel to stagnate and decompose in this region. The catalyst beds were of cylindrical geometry for ease of loading. The engine was designed for all-welded construction, and provisions were made to incorporate an expansion skirt on the nozzle.

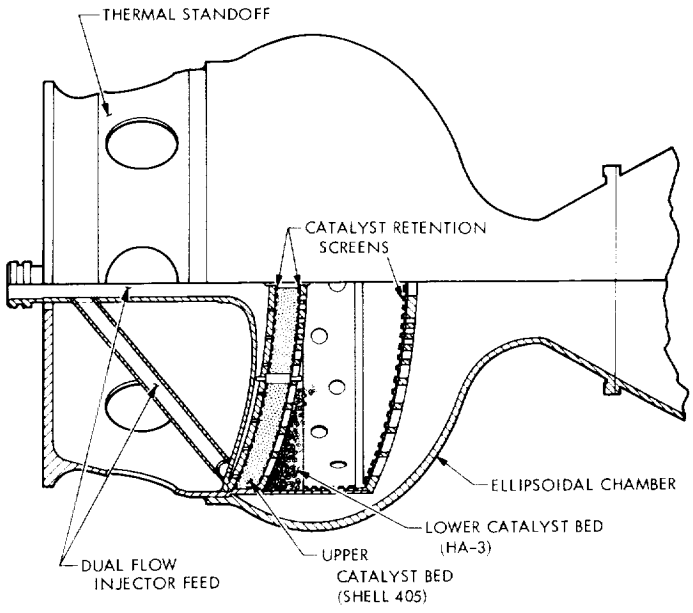

Fig. 28. Advanced lightweight throttleable N_2H_4 engine design

Table 6. Advanced lightweight engine design parameters

Parameter	Value
Thrust	2670 N (600 lb_f)
Weight (estimated) loaded, less valve	4.7 kg (10.4 lb_m)
Catalyst: 2 layered beds	
Upper: 14-18 mesh Shell 405 pellets	100 g (0.22 lb_m)
Lower: 3.2-mm (1/8-in.) HA3 pellets	520 g (1.15 lb_m)
Life (estimated)	>1500 s
Catalyst bed diameter	144 mm (5.6 in.)
Catalyst bed depth: upper	7.6 mm (0.3 in.)
lower	38 mm (1.5 in.)
Chamber pressure	1.379 MN/m^2 (200 psia)
Bed loading at full thrust	77 kg/m^2-s (0.11 $lb_m/in.^2$-s)
Chamber geometry	Elliptical
Chamber material	L 605
Throat diameter	38.43 mm (1.513 in.)
Estimated throttling range	10/1

VII. Conclusions and Recommendations

There appear to be no problems of a fundamental nature associated with the steady-state operation or dynamic throttling of large (2670 N, 600 lb_f) monopropellant hydrazine reactors, and none which should in any way preclude the use of throttled monopropellant hydrazine thrusters on planetary lander missions. The minor problems uncovered in this evaluation centered about details of mechanical design, materials of construction, and fab-

rication and joining techniques, and were readily amenable to engineering solution. They were no more serious than similar problems typically encountered with monopropellant hydrazine reactors of smaller size.

Both high-thrust throttleable thrusters evaluated delivered what was deemed satisfactory dynamic throttling performance in response to sinusoidal and square-wave input signals, although what is considered "satisfactory" depends upon the standard of comparison. Optimum system response was found to be very sensitive to adjustments in the valve drive amplifier.

Heat sterilization of reactors containing beds of Shell 405 catalyst has little effect on engine characteristic velocity, but would probably increase the length of the first reactor start transient somewhat. The quantity of Shell 405 catalyst needed may be reduced by using a stratified bed comprising an upstream layer of Shell 405 and a downstream layer of a nonspontaneous catalyst such as HA3. This results in a slight increase in the start transient, but appears to give smoother combustion than can be attained with beds of all 405 Shell catalyst; characteristic velocity is unaffected. The use of injectors which uniformly distribute a large number of finely divided propellant streams across the catalyst bed at close range results in smoother combustion than when the streams must traverse an intervening void space or gap before contacting the catalyst.

This work has demonstrated that existing catalyst bed and monopropellant reactor design criteria may be successfully extended and applied to the design and operation of high-thrust throttleable hydrazine reactors. The results of the subscale experiments point out, however, that our understanding of the internal ballistics of catalyst beds on a fundamental level is still incomplete. The use of existing design criteria does not *a priori* guarantee that catalyst-related phenomena, such as "washout," will not occur. Further work to definitize catalyst bed internal ballistics for the purpose of complete prediction and control of reactor behavior is believed to be warranted.

Because planetary lander engines were originally envisioned as the most likely end application of throttleable hydrazine thruster technology, 500 s was selected as the engine life design goal in this program. The lightweight engine tested actually accumulated in excess of 1500 s duration, with no apparent degradation in performance. Although there seems to be no reason to doubt that still greater useful engine life is attainable with the present state of the technology, engine lifetimes greater than about 1500 s cannot be guaranteed with confidence. It is recommended that further experimentation be conducted to establish design criteria for long engine life if high-thrust (2224-13,344 N, 500–3000 lb_f) catalytic monopropellant hydrazine thrusters are ever considered for applications where long useful service life is an important requirement.

Nomenclature

A_c cross-sectional area of chamber

c^* characteristic velocity

G bed loading (mass flow rate/cross-sectional area)

m mass flow rate

V_i command voltage to valve

P_c chamber pressure

ΔP_c variation in chamber pressure (used to determine chamber pressure roughness)

P_{c_i} instantaneous chamber pressure

$P_{c_{ss}}$ steady-state chamber pressure

ε expansion area ratio (area of nozzle exit/area of nozzle throat)

ΔP_{c_i} instantaneous variation in chamber pressure (used to determine amplitude ratio)

$\Delta P_{c_{ss}}$ steady-state variation in chamber pressure (used to determine amplitude ratio)

References

1. *Voyager Capsule Preliminary Design, Phase B*, Vols. I–V, Martin-Marietta Corp., Denver, Colo., Aug. 31, 1967.

2. *Study of Direct vs Orbital Entry for Mars Missions*, Vols. 1–6, Martin-Marietta Corp., Denver, Colo., Aug. 1968.

3. Groudle, T. A., "Sterilizable Liquid Propulsion System Development," *Supporting Research and Advanced Development*, Space Programs Summary 37-47, Vol. III, pp. 153–158, Jet Propulsion Laboratory, Pasadena, Calif., Oct. 31, 1967.

4. Kenny, R. J., and Reeves, D. F., *Final Report, Throttleable Thruster System*, JPL Contract 952344, TRW Systems Group, Redondo Beach, Calif., Apr. 28, 1970.

5. Kenny, R. J., and Reeves, D. F., "Throttled Thruster System Design, Fabrication, and Test Verification," Paper 70-652, presented at the AIAA Sixth Propulsion Joint Specialist Meeting, San Diego, Calif., June 17, 1970.

6. Price, T. W., "High-Thrust Throttleable Monopropellant Hydrazine Reactors," *Supporting Research and Advanced Development*, Space Programs Summary 37-66, Vol. III, pp. 213–221, Jet Propulsion Laboratory, Pasadena, Calif., Dec. 31, 1970.

7. Price, T. W., "Long-Duration Firings of a Mariner Mars 1969 Catalytic Reactor," *JPL Quarterly Technical Review*, Vol. 1, No. 3, pp. 57–66, Jet Propulsion Laboratory, Pasadena, Calif., Oct. 1971.

8. Price, T. W., "Experimental Evaluation of High-Thrust, Throttleable Monopropellant Hydrazine Reactors," Paper 71-705, presented at the AIAA/SAE Seventh Propulsion Joint Specialist Conference, Salt Lake City, Utah, June 14–18, 1971.

9. *Mariner Mars 1969 Final Project Report: Development, Design, and Test*, Technical Report 32-1460, Vol. I, p. 398, Jet Propulsion Laboratory, Pasadena, Calif., Nov. 1, 1970.

10. *Surveyor Project Final Report, Part 1. Project Description and Performance*, Technical Report 32-1265, Vol. II, Jet Propulsion Laboratory, Pasadena, Calif., July 1, 1969.

11. Reeves, D. F., *Final Report Addendum, Throttleable Thruster Systems*, JPL Contract 952344, TRW Systems Group, Redondo Beach, Calif., May 29, 1971.

12. Fitzgerald, A. E., and Higginbotham, D. E., *Basic Electrical Engineering*, Second Edition, McGraw-Hill Book Co., Inc., New York, 1957.

13. Sangiovanni, J. J., and Kesten, A. S., "Motion Picture Studies of the Startup Characteristics of Liquid Hydrazine Catalytic Reactors," paper presented at the AIAA/SAE Seventh Propulsion Joint Specialist Conference, Salt Lake City, Utah, June 14–18, 1971.

14. Grant, A. F., Jr., *Basic Factors Involved in the Design and Operation of Catalytic Monopropellant-Hydrazine Reaction Chambers*, Report 20-77, Jet Propulsion Laboratory, Pasadena, Calif., Dec. 1954.

References (contd)

15. Kesten, A. S., *Analytical Study of Catalytic Reactors for Hydrazine Decomposition – Second Annual Progress Report*, UARL G 910461-24, Research Laboratories, United Aircraft Corp., East Hartford, Conn., May 1968.

16. *Development of Design and Scaling Criteria for Monopropellant Hydrazine Reactors Employing Shell 405 Catalyst, Final Report*, Report RRC-66-R-76, Vol. II, Rocket Research Corp., Redmond, Wash., Jan. 18, 1967.

NASA — JPL — Coml., L.A., Calif.